



## A Robust PID Power System Stabilizer Design of Single Machine Infinite Bus System using Firefly Algorithm

Zakirhussain FARHAD<sup>1,\*</sup>, Ibrahim EKE<sup>2</sup>, Suleyman Sungur TEZCAN<sup>3</sup>, Shah Jahan SAFI<sup>4</sup>

<sup>1,4</sup> Department of Power Engineering, Electro-mechanic faculty, Kabul polytechnic university, Kabul, Afghanistan

<sup>2</sup> Department of electrical and electronics, faculty of Engineering, Kirikkale university, Kirikkale, Turkey

<sup>3</sup> Department of electrical and electronics, faculty of Engineering, Gazi university, Ankara, Turkey

### Article Info

Received: 24/11/2017

Accepted: 23/12/2017

### Keywords

Conventional power system stabilizer  
Firefly algorithm  
optimized PID based PSS  
Bat algorithm optimized conventional PSS  
SMIB power system

### Abstract

This paper presents the design of a proportional-integral-derivative power-system-stabilizer using the firefly algorithm for tuning of stabilizer parameters and washout (reset). The proposed optimization of parameters is carried out with eigenvalue analysis based objective function for two cases (two parametric bounds) to guarantee the stability for the single-machine-infinite-bus system model for a wide range of operating conditions. The system performance with Firefly-Algorithm tuned controller is compared with Bat-Algorithm optimized Conventional-Power-System-Stabilizer controller. The power system robustness is tested on 133 operating conditions to set up the superior performance of FA-PID-PSS over the BA-CPSS. According to the eigenvalue analysis and time response parameters results, it is found that BA-CPSS and FA-PID-PSS (case-I) have the ability to stabilize the system for some operating conditions; but the FA-PID-PSS (case-II) can stabilize the system and can improve settling time and overshoot for all operating conditions..

## 1. INTRODUCTION

The excitation control of generators is among the important topics in the field of power system. A good excitation control is the best way to damp the oscillations and improve the rotor angle stability of generators [1]. Using power system stabilizer (PSS) is a superior method to improve the damping of rotors electromechanical oscillations and in line it enhances the transmission lines energy transfer capability. It provides the damping for developing the component of electrical torque in phase with the deviations of rotor speed by modulating the voltage reference of exciter control [2].

Power system stabilizers are successfully used in power systems for few years because of their flexibility low cost and easy implementation. In existing power system the conventional power system stabilizers are used in wide range and have contributed to enhance the dynamic stability of power systems [3]. This kind of damping torque production is the most efficient procedure to enhance small signal stability of power systems, in comparison to Flexible AC Transmission System (FACTS) - based controllers [3]. Moreover, a supplementary controller may be designed for each FACTS device and these electronic devices are not directly involved with electromechanical oscillations. As a result, the damping controller (FACTS) design is not as straightforward as those of the PSS [1].

Different types of controllers like Proportional plus Derivative (PD), Proportional plus Integral (PI), Proportional plus Derivative plus Integral (PID) and Lead Lag controllers were designed to stabilize the system. Lead Lag controllers which is characterized by its simple implementation are the traditional type of controllers. PID which is a combination of proportional, derivative and integral is the leading type of

\*Corresponding author, e-mail: zakirhussainfar@kpu.edu.af

controllers. It computes the error between the desired and the measured variables and tries to reduce the error by tuning the input parameter [4].

The power system and control engineers made an important contribution to conventional power system stabilizer design after the initial work of Concordia and deMello [5]. After that, the most models were developed by using advanced and new control hypothesis such as optimal control, eigenvalue (pole) assignment [6] and adaptive control [7]. The PSS structure selection and design is a complicated process of iteration. The better power system stabilizer design, to be capable for adapting each variation according to the changing of operational condition can be performed by self-tuning [6], such as adaptive control methods based on Lyapunov [8] for the design of PSS. For this kind of methods, it is necessary to know extensive knowledge of power system dynamics and require a long time for processing [9].

To improve the performance of power system stabilizer many techniques have been proposed to design PSSs parameters for example population based such as Artificial Bee Colony (ABC) algorithm [10], Artificial Neural Networks (ANNs) as in [11], fuzzy logic in [12–16], adaptive fuzzy in [17,18], neuro-fuzzy in [19–21] and many other intelligent optimization techniques. From last few years fuzzy logic controller is used in power system applications as a powerful tool.

In [22], by Bat-Algorithm optimized novel fractional order PID-PSS is suggested that has been tested on a SMIB power system under different disturbances and operating conditions. In [23], a robust PID-based PSS is suggested to appropriately function over a wide range of operating conditions. Doubts in plant parameters, due to deviation in load patterns and generation, are expressed in the form of a poly topic structure. The problem of PID control is initially reduced to a generalized static output feedback synthesis. In [24], the authors proposed a simple analytical method to compute the set of three terms of robust stabilizing PSSs. Thus, stabilization of the proposed interval plant by a PID controller and a phase lead compensator based PSS is dealt with using generalized Kharitonov's theorem. Besides, essential and satisfactory constraints for characterizing the robust stabilizing three term controllers are derived by applying the Routh–Hurwitz criterion to a set of segment/vertex plants.

Therefore, Particle Swarm Optimization, PSO algorithm is one of the robust optimization methodologies in the procedure of solving the best PID controller parameters problem. As in [25], an optimal PSO based PID PSS is proposed, which utilizes the speed deviation as the input. In [26], a design method for the stability improvement of a SMIB power system using PID-PSS has been developed, in which its parameters are optimized by Hybrid Particle Swarm-Bacteria Forging Optimization (PSBFO) technique. A real coded GA based PID is produced in [27] for improving the power system dynamic, in which the proposed stabilizer's parameters are adjusted by using real coded GA.

In this study a PID based PSS controller is considered and at nominal operational condition tuned for two cases of parametric bounds using Firefly Algorithm (FA) and examined them on a huge range of operational conditions (133 different conditions). Moreover, the rest of this paper is arranged as follows; Part-II deals with the power system mathematical modeling for SMIB power system. In Part-III is 'PID based Power System Stabilizer Tuning' followed by the eigenvalue based objective function, review on the Firefly algorithm and its parameter setting. In Part-IV is 'Results and discussion' followed by the comparative performance analysis of FA-PID-PSS (case-II) (proposed), FA-PID-PSS (case-I) and BA-CPSS is achieved, in terms of speed response (overshoot and settling time), and eigenvalue based analysis to guarantee the robustness of PSS for 133 conditions. In Part-V is 'Conclusion' then followed by appendix, nomenclature and at the end references.

## 2. POWER SYSTEM MODELING AND PID-PSS TUNING

The SMIB system model as shown in Figure 1, is used to evaluate the performance of power system stabilizer. Where  $R_e$  and  $X_e$  are in order the transmission line resistance and reactance. The  $E_b$  and  $V_t$  are infinite bus voltage and terminal voltage of generator respectively. In figure 1, the switches  $S_1$ ,  $S_2$  and  $S_3$  are used to change the kind of PSSs during the power system test for comparing them. BA based PSS form, Firefly based PID-PSS form and without PSS form are shown in the power system model [28].

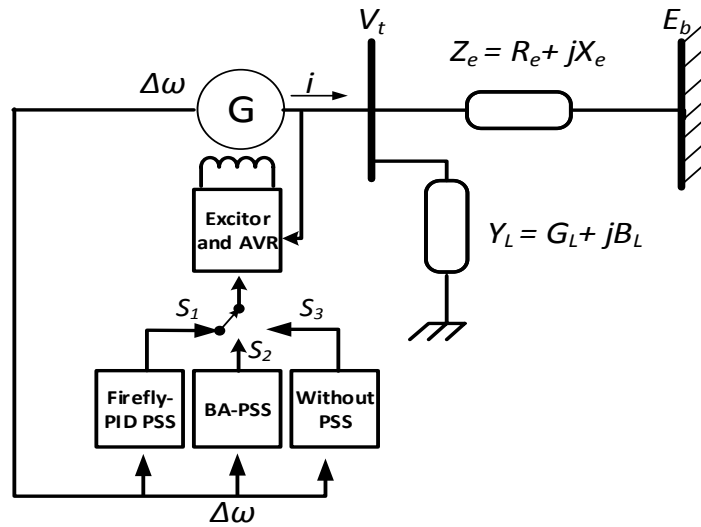


Figure 1. System configuration. Single machine infinite bus with PSSs.

### 2.1. Non-linear Model

As shown in Figure.1, the non-linear model is developed by making use of the generator third order model and using IEEE's type-1 exciter model is shown in Figure. 2. The complete modeling is represented with equations (1) - (4),

$$\dot{\omega} = \frac{1}{M}(T_m - T_e - T_D) \tag{1}$$

$$\dot{\delta} = \omega_b(\omega - 1) \tag{2}$$

$$\dot{e}'_q = \frac{1}{T'_{d0}} [E_{FD} - e'_q - (x_d - x'_d)] \tag{3}$$

$$\dot{E}_{FD} = \frac{1}{T_A} [K_A(V_{ref} - v_{dt} + u_{PSS}) - E_{FD}] \tag{4}$$

where  $\delta$  is the rotor angle in rad,  $\omega$  is the generator speed in rad/s,  $e'_q$  is the generator voltage in q-axis and  $E_{FD}$  is the output voltage of exciter.  $T_m$ ,  $T_e$  and  $T_d$  are the mechanical, electrical and damping torque respectively.  $x_d$  and  $x'_d$  is generator's synchronous reactance and transient reactance in d-axis,  $v_t$ ,  $V_{ref}$  and  $u_{PSS}$  are the terminal, reference and power system stabilizer output voltages respectively.  $T_A$  and  $T'_{d0}$  are the time constants of the exciter and generator model.

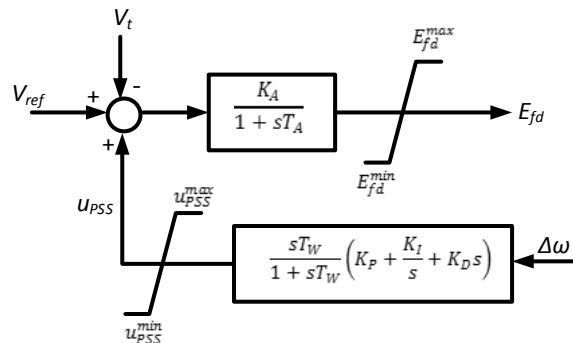


Figure 2. IEEE type-1 exciter model with PID-PSS.

### 2.2. Linear Model

As in section-1 the non-linear model is linearized using the Phillips-Heffron model as in Figure 3. In state-space form, the open-loop system is

$$\begin{bmatrix} \dot{\Delta\delta} \\ \dot{\Delta\omega} \\ \dot{\Delta e_q} \\ \dot{\Delta E_{fd}} \end{bmatrix} = \begin{bmatrix} 0 & \omega_b & 0 & 0 \\ -\frac{K_1}{M} & -\frac{D}{M} & -\frac{K_2}{M} & 0 \\ -\frac{K_4}{T'_{do}} & 0 & -\frac{K_3}{T'_{do}} & \frac{1}{T'_{do}} \\ -\frac{K_A K_5}{T_A} & 0 & -\frac{K_A K_6}{T_A} & -\frac{1}{T_A} \end{bmatrix} \begin{bmatrix} \Delta\delta \\ \Delta\omega \\ \Delta e_q \\ \Delta E_{fd} \end{bmatrix} + \begin{bmatrix} 0 \\ 0 \\ 0 \\ \frac{K_A}{T_A} \end{bmatrix} u_{PSS} \tag{5}$$

Where,  $K_1$ - $K_6$  are constants.

### 2.3. Control Strategy

In present work, the Proportional Integral Derivative based Power System Stabilizer (PID-PSS) controller is proposed and placed in a feedback loop with a washout as shown in Fig. 4. It is one of the most powerful but made up of interconnected parts controller mode combines the proportional, integral and derivative mode. The offset of the proportional mode is eliminated by this mode and it supplies fast response [29].

### 2.4. Composite Linear Model

To have the composite linear model in the form of Eq. (6), by a small disturbance the states of the non-linear model are perturbed,

$$\begin{cases} \dot{x} = Ax + Bu \\ y = Cx + Du \end{cases} \tag{6}$$

where, the matrix  $A$  is a composite of the perturbed states  $[\Delta\omega \ \Delta\delta \ \Delta e_q \ \Delta E_{FD} \ x_5]^T$ ,  $u$  is the control composed of  $u_{PSS}$ , while matrix  $C$  is the required output from the system. In this work the output is rotor speed deviation  $\Delta\omega$ . The matrix  $D$  is adjusted to be zero.

### 2.5. Closed loop system

The compound linear model that developed in matrix  $B$  is modeled in the form of Eq. (7) as a closed loop system,

$$\dot{Z} = A_c Z \tag{7}$$

where,  $Z$  is composed of  $[\Delta\omega \ \Delta\delta \ \Delta e_q \ \Delta E_{FD} \ x_5 \ u_{PSS}]^T$  and  $A_c$  is the closed loop matrix. The overall closed loop matrix  $A_c$  then can be written as,

$$\begin{bmatrix} 0 & \omega_b & 0 & 0 & 0 & 0 \\ -\frac{K_1}{M} & 0 & -\frac{K_2}{M} & 0 & 0 & 0 \\ \frac{K_4}{T'_{do}} & 0 & -\frac{1}{T'_{do}K_3} & \frac{1}{T'_{do}} & 0 & 0 \\ -\frac{K_A K_5}{T_A} & 0 & 0 & -\frac{1}{T_A} & 0 & \frac{K_A}{T_A} \\ -\frac{K_1}{M} & 0 & 0 & 0 & -\frac{1}{T_w} & 0 \\ \frac{K_1 K_D}{MT_w} - \frac{K_1 K_P}{M} + \frac{K_2 K_4 K_D}{MT'_{do}} & \frac{-K_1 K_D \omega_b}{M} & \frac{K_2 K_D}{MK_3 T'_{do}} + \frac{K_2 K_D}{MT_w} - \frac{K_2 K_P}{M} & \frac{-K_2 K_D}{MT'_{do}} & \frac{K_D + (K_I T_w - K_P) T_w}{(T_w)^2} & 0 \end{bmatrix} \tag{8}$$

where,  $K_P$ ,  $K_I$  and  $K_D$  are proportional, integral and derivative, PID parameters respectively [30].

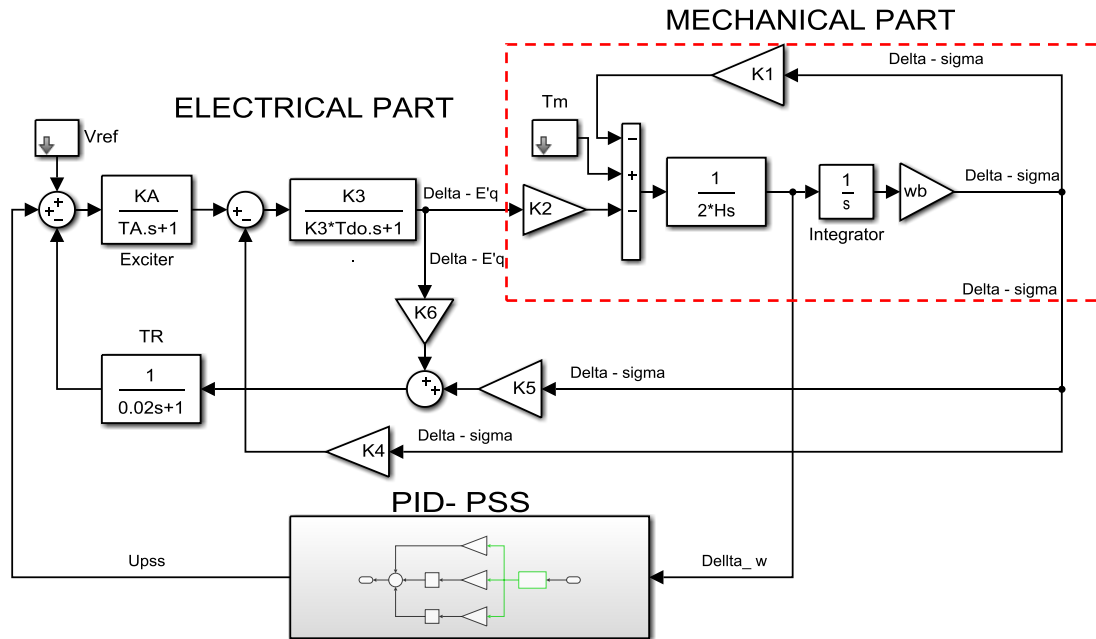


Figure 3. Linearized Phillips-Heftron model showing the electrical and mechanical loops.

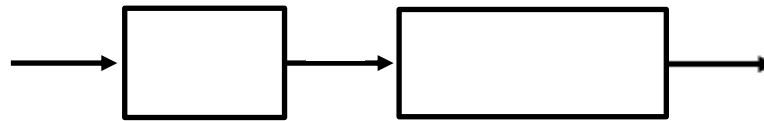


Figure 4. PID based PSS controller consisting of wash-out Filter

### 3. PID-PSS TUNING

#### 3.1. Objective Function

A robust tuning should be incorporated for increasing the damping of a power system configuration over a broad range operating conditions. So, the design of PSS is formulated as eigenvalues based objective function. The maximization of damping factor based and eigenvalue real part minimization based two sub-objective functions are considered as in [31]. These are represented by Eqs. (9) and (10).

$$J_1 = \min[\text{Real}(\lambda_i); \lambda_i \in \text{oscillatory modes}] \tag{9}$$

$$J_2 = \max[\xi_i; \xi_i \in \xi \text{ of oscillatory modes}] \tag{10}$$

where,  $\xi_i$  is eigenvalue damping ratio for the  $i$ th electromechanical mode and  $\text{Real}(\lambda_i)$  is the real part of eigenvalue for the  $i$ th electromechanical mode. The purpose of optimization for  $J_1$  is to replace the lightly damped eigenvalues to the left side of  $s$ -plane. The  $J_2$  is increased to augment the damping of electromechanical mode oscillations. The limits for the optimization are the bounds on the parameters that to be optimized like PID parameters and the washout time constant. Therefore, the optimization problem is subjected to

$$K_p^{min} \leq K_p \leq K_p^{min} \tag{11}$$

$$K_I^{min} \leq K_I \leq K_I^{min} \tag{12}$$

$$K_D^{min} \leq K_D \leq K_D^{min} \tag{13}$$

$$T_w^{min} \leq T_w \leq T_w^{min} \tag{14}$$

For the PID parameters to be optimized the limits values are taken as [0 - 50] for  $K_P$ , [0 - 50] for  $K_I$ , [0 - 10] for  $K_D$  and [0 - 50] for  $T_w$  in case one and [0 - 300] for  $K_P$ , [0 - 500] for  $K_I$ , [0 - 100] for  $K_D$  and [0 - 50] for  $T_w$  in case two. To determine the damping ratio for the  $i^{th}$  critical mode, Eq. (15) is used,

$$\xi_i = \frac{-\sigma_i}{\sqrt{\sigma_i^2 + \omega_i^2}} \tag{15}$$

where considered eigenvalue is given by  $\lambda_i = \sigma_i \pm \omega_i$ . Therefore, the objective functions can be given as

$$J_1 = \sum_{i=1}^n (\sigma_0 - \sigma_i)^2 \tag{16}$$

$$J_2 = \sum_{i=1}^n (\xi_0 - \xi_i)^2 \tag{17}$$

where  $\sigma_i \leq \sigma_0$  and  $\xi_i \geq \xi_0$  for  $i = 1, 2 \dots, n$ . The effect of  $J_1$  and  $J_2$  are shown in Figure 5(a. and .b), correspondingly. While the combined objective function  $J = J_1 + \alpha J_2$  is able to place the eigenvalue of closed loop system in the s-plane D-shape sector as in Figure 5(c). The value of  $\alpha$  is considered 10.

### 3.2. Firefly Algorithm

FA is based on fireflies' behavior and the flashing patterns. Essentially, the following three idealized rules are used by FA:

- A firefly will be attracted to other fireflies without any regard of their sex, because fireflies are unisex.
- The attractiveness and the brightness are proportional to each other, and when their distance increases they both decrease. So for any two flashing fireflies, the less bright firefly will start movement towards the brighter one. The firefly will move by chance (randomly) if there is no brighter one than a specific firefly.
- The landscape of the objective function determines the brightness of a flashing firefly.

As the attractiveness of a firefly is proportional to the light intensity seen by the nearest fireflies, in such a case the variation of attractiveness  $\beta$  with the distance  $r$  can define by

$$\beta = \beta_0 e^{-\gamma r^2}, \tag{18}$$

where  $\beta_0$  is the attractiveness at  $r = 0$ .

To more attractive (brighter) firefly  $j$  the movement of attractiveness of a firefly  $i$  is given by

$$x_i^{t+1} = x_i^t + \beta_0 e^{-\gamma r_{ij}^2} (x_j^t - x_i^t) \tag{19}$$

where the 2<sup>nd</sup> expression is because of the attractiveness. The 3<sup>rd</sup> expression is randomization with the parameter of randomization  $\alpha_t$ , and  $\epsilon_i^t$  is a random numbers vector drawn at time t from a uniform distribution or Gaussian distribution. If  $\beta_0 = 0$  it will become a simple random walk. Form another point of view, if  $\gamma = 0$ , it decreases a variant of particle swarm optimization [32]. Moreover, the randomization  $\epsilon_i^t$  can be easily expanded to other distributions like Lévy flights [32 and 33].

### 3.3. Parameter Settings

As the randomness is essentially controlled by  $\alpha_t$ , during iterations this parameter can be tuned, therefore it can vary by the iteration counter t. thus a better choice for expressing  $\alpha_t$  is using of

$$\alpha_t = \alpha_0 \delta^t, \quad (0 < \delta < 1), \tag{20}$$

where  $\alpha_0$  is the scaling factor of initial randomness, and  $\delta$  is significantly a cooling factor. On the various applications,  $\delta = 0.95$  to  $0.97$  can be used [32].

According to the initial  $\alpha_0$ , if  $\alpha_0$  is associated with the scaling of design variables, firefly will work efficiently. Let consider  $L$  be the mean scale of the interest problem,  $\alpha_0 = 0.01L$  can be set as an initial value. The X. S. Yang reported that the 0.01 factor is the original value that a random walks needs a number of steps to achieve the goal while balancing the local exploitation without jumping too far in a few steps [34, 35].

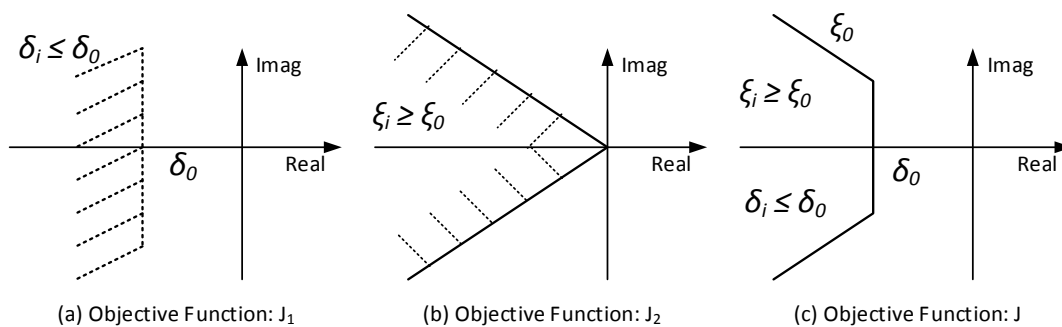


Figure 5. Illustration of objective function.

The attractiveness is controlled by the parameter  $\beta$ , and from the suggestion of parametric studies that for various applications  $\beta_0 = 1$  can be used. However,  $\gamma$  should be also related to the scaling  $L$ . In general, we can set  $\gamma = 1/\sqrt{L}$ . If the variations of scaling are not essential, then we can select  $\gamma = O(1)$ . For various applications, the population size  $n = 15$  to  $100$  can be used, though  $n = 25$  to  $40$  is the best range for usage [32, 34].

## 4. RESULT AND DISCUSSION

### 4.1. The Creation of Experimental Conditions

The configuration of the SMIB power system is shown in Figure 1 and the data of power system is in Appendix A. The speed of generator that is used as input of the PSS sensing from the shaft and the output of power system stabilizer is applied to the Automatic Voltage Regulator (AVR) at the reference voltage junction. In this work, the consideration of test power system to be operated is within the ranges of real power and the transmission line reactance as shown in Figure 1, are given in Eqs. (21) and (22).

$$0.4 \leq P_{g0} \leq 1.3 \quad (21)$$

$$0.2 \leq X_e \leq 0.5 \quad (22)$$

The power system operating point involves all practical operational conditions as mentioned above and generating a range of 133 different operational conditions. In this study, as shown in Table 1 from 133 operating conditions only eight have been considered for time domain analysis of the power system. These eight sample operating conditions are pointed out in terms of line reactance and active power in pu and related eigenvalues, damping ratios and oscillations frequency. More than 0.1 is the favored damping ratio as in [36] and the eigenvalues location must be in the LHS of the s-plane to guarantee the stability conditions; consequently, operating conditions 6–8 demonstrate a power system unstable state [9].

#### 4.2. PID-PSS Parameters Optimized by Firefly Algorithm

The MATLAB environment is used to obtain the effectiveness of the proposed FA-PID-PSS algorithm. The algorithm parameters utilized for simulations are:  $Iter = 30$ ;  $n = 40$ ;  $\gamma = 1$ ;  $\beta_0 = 2$ ;  $\alpha = 0.2$ ;  $\alpha_{damp} = 0.99$ ;  $\delta = 0.05(Var_{max} - Var_{min})$ ;  $m = 2$ . For optimal tuning of PID-PSS parameters, we considered the operating of SMIB system at nominal operational condition (in which  $X_e = 0.4 pu$  and  $P = 1.0 pu$ ); subjected to the objective function based on eigenvalues with the parametric two limits cases such as  $0 \leq K_p \leq 50$ ,  $0 \leq K_I \leq 50$ ,  $0 \leq K_D \leq 20$  and  $0 \leq T_w \leq 50$  for case-1 and  $0 \leq K_p \leq 300$ ,  $0 \leq K_I \leq 500$ ,  $0 \leq K_D \leq 100$  and  $0 \leq T_w \leq 50$  for case-2. For nominal operating condition of system the optimized parameters are enlisted in Table. 2. The performance of tuned FA-PID-PSS with the SMIB system is checked and compared to CPSS tuned by BA as shown in [9], the tuned parameters are pointed out in Table 3. In the section of Simulation results the comparison performance is presented.

#### 4.3. Eigenvalue Analysis

##### 4.3.1. Test system without PSS

In this part, the nature of SMIB system for the range of 133 different operational conditions by using eigenvalues plot on s-plane is analyzed. The entire range of operating conditions as given by Eqs. (21) and (22) with 0.05 step size, outcomes to be 133. For these operating conditions without power system stabilizer (under open loop) the corresponding eigenvalues plot is represented in Figure-6. With the increase in line reactance  $X_e$  and also in active power  $P_{g0}$  the corresponding eigenvalue replaces to the RHS of s-plane. In the result of the case, where, the PSS isn't added to the system; 61 operating conditions are unstable by the cause of eigenvalues position in RHS of s-plane and 72 operating conditions are stable due to the corresponding eigenvalues location in left hand side (LHS) of s-plane. The stability and instability for mentioned operating conditions are pointed out in Table 4. If the eigenvalues of electromechanical mode located in the s-plane D-shape sector, the system stability will be guaranteed [9], accordingly, the preferred damping ratio grid as 0.1 is considered and to confirm D-shape sector on the s-plane the eigenvalues are plotted on the figure. As indicated in the plot of Figure 6, that the eigenvalues of system for 61 operating conditions are not located in s-plane D-shape sector therefor representing instability which call to use the optimized PSS with the power system.

##### 4.3.2. Test system with FA tuned PID-PSS

As obtained in 'Test system without PSS', that 72 operating conditions without PSS satisfy the stability conditions but not located in s-plane D-shape sector to guarantee the system stability. Thus, the PID based PSS is used with the generator of the test system, and for the two parametric bounds (case-I and II) using FA its tuning is carried out with objective function based on eigenvalues. The optimized controllers of SMIB system as pointed out in Table 2 are subjected to eigenvalue plot and shown in Figure 7 and Figure 8. For the case-I, the eigenvalue plots for 126 operating conditions with tuned PID-PSS, are located in s-plane D-shape sector and for the case-II the eigenvalue plots of all 133 operating conditions with tuned



PID-PSS, are located in s-plane D-shape sector. The adjusted eigenvalues, damping ratios and frequencies of the system with FA-PID-PSS (case-I and II) for the sample operating conditions (in number 1 to 8 as in Table 1) are pointed out in Table 5. It is obvious that for the system with FA-PID-PSS (case-I) neither real part of eigenvalues are positive nor damping ratios are less than 0.1, ensuring stability condition in s-plane D-shape sector.

**Table 1.** For operating conditions 1–8 of without PSS system eigenvalues, damping ratios and oscillatory frequency of the electro- mechanical modes.

Sample operating condition	Active Power	Line Reactance	Eigenvalues	Damping Ratio	Frequency (Hz)
Condition -1	0.5	0.2	$-0.7868 \pm 6.3423i$	0.1231	1.017
Condition -2	0.5	0.4	$-0.4881 \pm 5.5579i$	0.0875	0.888
Condition -3	0.75	0.2	$-0.5246 \pm 7.3978i$	0.0707	1.18
Condition -4	0.75	0.4	$-0.1728 \pm 6.5099i$	0.0265	1.036
Condition -5	1.0	0.2	$-0.1073 + 7.9336i$	0.0135	1.262
Condition -6	1.0	0.4	$0.3906 + 7.0415i$	-0.0554	1.122
Condition -7	1.2	0.4	$0.9185 + 7.8742i$	-0.1180	1.163
Condition -8	1.3	0.2	$0.3979 + 8.2132i$	-0.0484	1.308

**Table 2.** Firefly algorithm based optimized parameters of PID-PSS

Controller	$K_p$	$K_i$	$K_d$	$T_w$
FA-PID-PSS, case-I	22.0607	30.4979	4.0506	27.8732
FA-PID-PSS, case-II: Proposed	198.0827	477.561	28.422	39.5729

#### 4.3.3 Test system with BA-CPSS

In this test system the BA-CPSS as proposed by D.K. Sambariya, R. Prasad [9] is use and the eigenvalue plot is shown in Figure 9. In the test performance, seven operating conditions eigenvalues located in the RHS of s-plane ( $3.7699 + 0.0000i$ ,  $3.7878 + 0.0000i$ ,  $3.8235 + 0.0000i$ ,  $3.7499 + 0.0000i$ ,  $3.7881 + 0.0000i$ ,  $3.8243 + 0.0000i$  and  $3.8583 + 0.0000i$  associated with  $X_e = 0.4:0.05:0.5$  pu,  $P = 1.15: 0.05: 1.3$  pu), indicating unstable mode of operation. Besides of it, with the most number of operating conditions the corresponding eigenvalues not taking place in the s-plane D-shape sector. The eigenvalues, damping ratios and frequency of chosen 8 sample operating conditions with BA-CPSS are obtain and illustrated in Table 5. It is mentionable that some of the damping factors associated with operating conditions are more than 0.1 but a few number are lesser than 0.1 and also smaller in magnitude as compared to power system with FA-PID-PSS (case-II). So, the ability of SMIB power system with FA-PID-PSS (case-II) (proposed) is better than the BA-CPSS [9].

**Table 3.** BA based optimized CPSS parameters: D.K. Sambariya, R. Prasad [9].

Controller	Gain: K	Zero: T1	Pole: T2	$T_w$
BA-CPSS:	20.1405	0.3017	0.0200	10

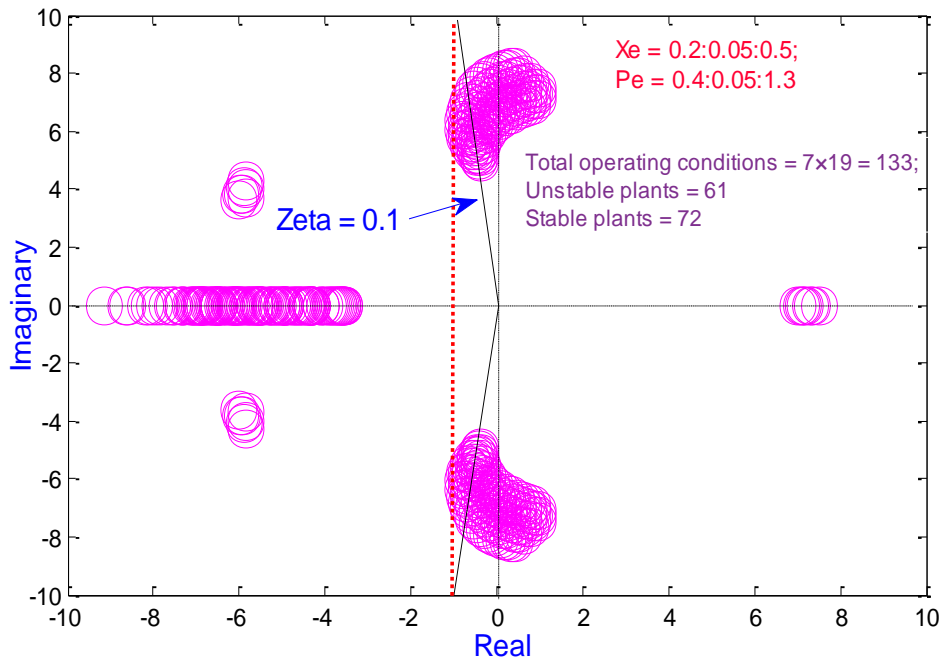


Figure 6. Eigenvalues plot of without CPSS based SMIB power system

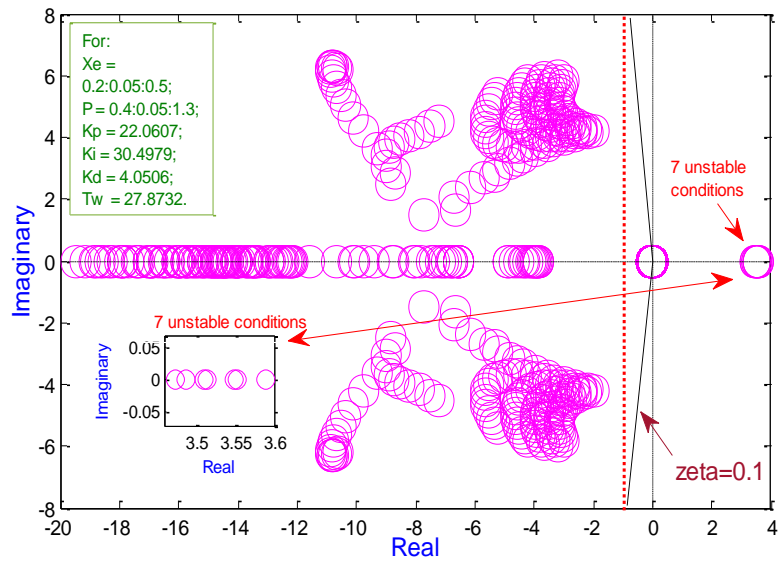


Figure 7. Eigenvalues plot of PID-PSS (case-I) based SMIB system

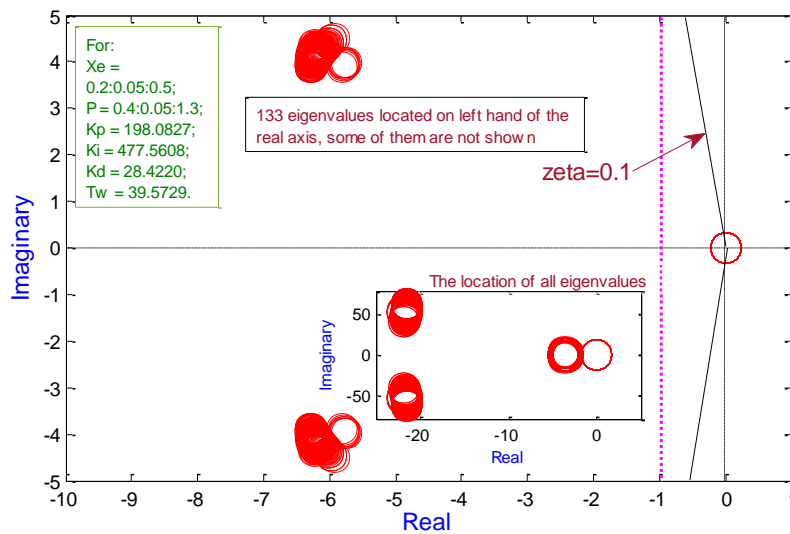


Figure 8. Eigenvalues plot of PID-PSS (case-II) based SMIB system

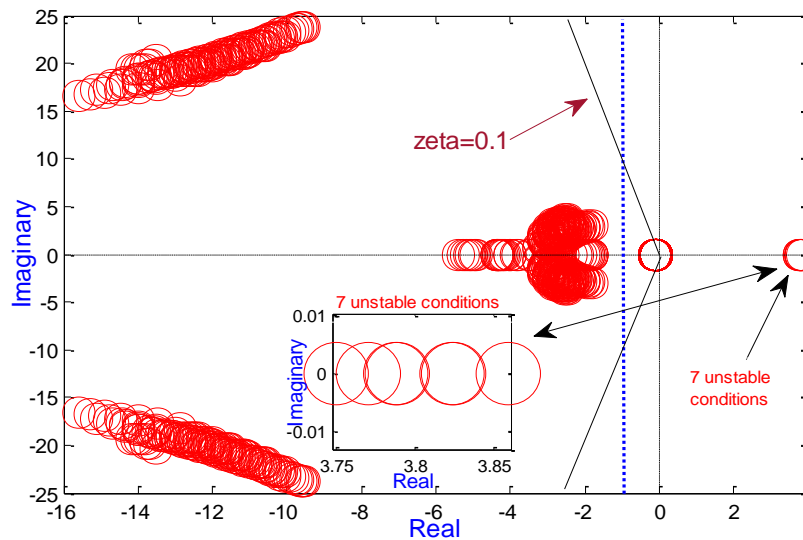


Figure 9. Eigenvalues plot of BA-CPSS [9] based SMIB system

Table 4. Eigenvalues based stable and unstable operating conditions for system without PSS, with BA-CPSS and with FA-PID-PSSs (case-I and II).

Xe	SMIB without PSS		SMIB with BA-CPSS [9]		SMIB with FA-PID_PSS(case-I)		SMIB with FA-PID_PSS(case-II)	
	Stable P	Unstable P	Stable P	Unstable P	Stable P	Unstable P	Stable P	Unstable P
0.20	0.40:0.05:1.05	1.10:0.05:1.3	All	Nil	All	Nil	All	Nil
0.25	0.40:0.05:0.95	1.10:0.05:1.3	All	Nil	All	Nil	All	Nil
0.30	0.40:0.05:0.90	0.95:0.05:1.3	All	Nil	All	Nil	All	Nil
0.35	0.40:0.05:0.85	0.90:0.05:1.3	All	Nil	All	Nil	All	Nil
0.40	0.40:0.05:0.80	0.85:0.05:1.3	0.40:0.05:1.25	1.3	0.40:0.05:1.251	1.3	All	Nil
0.45	0.40:0.05:0.75	0.80:0.05:1.3	0.40:0.05:1.20	1.25:0.05:1.3	0.40:0.05:1.20	1.25:0.05:1.3	All	Nil
0.50	0.40:0.05:0.75	0.80:0.05:1.3	0.40:0.05:1.10	1.15:0.05:1.3	0.40:0.05:1.10	1.15:0.05:1.3	All	Nil
Conditions	72	61	126	07	126	07	133	0

Table 5. Eigenvalues, damping ratios and oscillatory frequencies of the Electro-mechanical modes for sample operating conditions 1–8 with FA-PID-PSSs (case I, II) and BA-CPSS

Power system condition	PSS Model	Eigenvalues	Damping Factors	Frequency, Hz
Condition-1	FA-PID-PSS (case-I)	-6.6519 ± 1.6219i	0.9715	0.2581
	FA-PID-PSS (case-II)	-3.7521 ± 2.2929i	0.8533	0.3649
	BA-CPSS	-11.9730±19.9935i	0.5138	3.1821
Condition-2	FA-PID-PSS (case-I)	-2.8679 ± 4.1851i	0.5653	0.6661
	FA-PID-PSS (case-II)	-3.6043 ± 2.6572i	0.8049	0.4229

Condition-3	BA-CPSS	$-2.2548 \pm 2.5766i$	0.4295	0.4101
	FA-PID-PSS (case-I)	$-10.3483 \pm 5.0280i$	0.8995	0.8002
	FA-PID-PSS (case-II)	$-3.8116 \pm 2.2164i$	0.8645	0.3528
Condition-4	BA-CPSS	$-10.6369 \pm 22.3621i$	0.6492	2.9057
	FA-PID-PSS (case-I)	$-3.7428 \pm 4.5367i$	0.6364	0.7220
	FA-PID-PSS (case-II)	$-3.7095 \pm 2.5946i$	0.8194	0.4129
Condition-5	BA-CPSS	$-12.5598 \pm 19.823i$	0.5352	3.1549
	FA-PID-PSS (case-I)	$-10.8513 \pm 6.1431i$	0.8702	0.9777
	FA-PID-PSS (case-II)	$-3.8410 \pm 2.2321i$	0.8646	0.3552
Condition-6	BA-CPSS	$-9.9509 \pm 23.3392i$	0.3922	3.7145
	FA-PID-PSS (case-I)	$-3.9757 \pm 5.2319i$	0.6050	0.8327
	FA-PID-PSS (case-II)	$-3.7533 \pm 2.6496i$	0.8169	0.4217
Condition-7	BA-CPSS	$-11.8569 \pm 20.3102i$	0.5042	3.2325
	FA-PID-PSS (case-I)	$-3.9671 \pm 5.2309i$	0.6043	0.8325
	FA-PID-PSS (case-II)	$-3.7527 \pm 2.6507i$	0.8168	0.4219
Condition-8	BA-CPSS	$-11.8649 \pm 20.306i$	0.5045	3.2318
	FA-PID-PSS (case-I)	$-10.6095 \pm 6.1806i$	0.8641	0.9837
	FA-PID-PSS (case-II)	$-3.8532 \pm 2.3083i$	0.8578	0.3674
	BA-CPSS	$-9.5374 \pm 23.7947i$	0.3720	3.7870

#### 4.4. Simulation Results

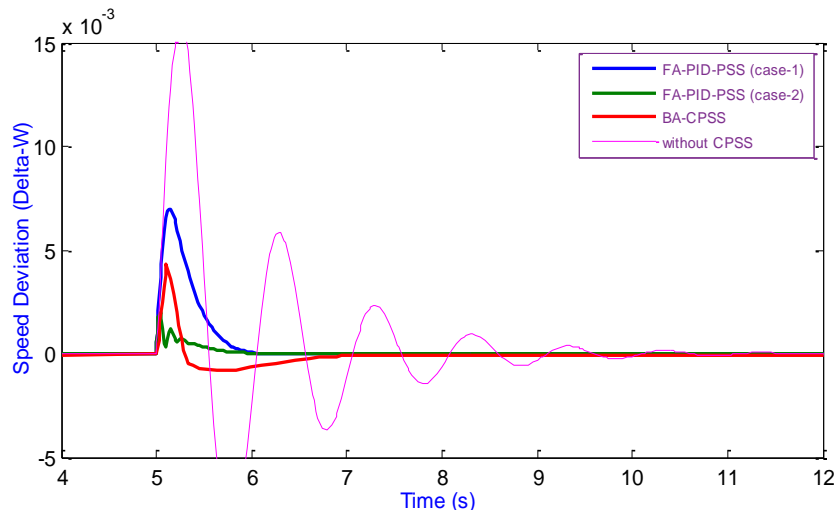


Figure 10. Speed response of without PSS, FA-PID-PSSs (case-I, II) and BA-CPSS based SMIB power system for Condition -1.

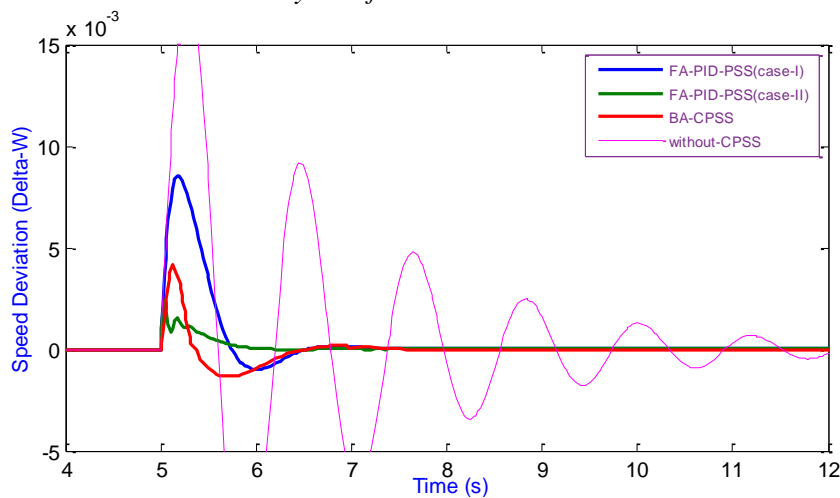


Figure 11. Speed response of without PSS, FA-PID-PSSs (case-I, II) and BA-CPSS based SMIB power system for Condition -2.

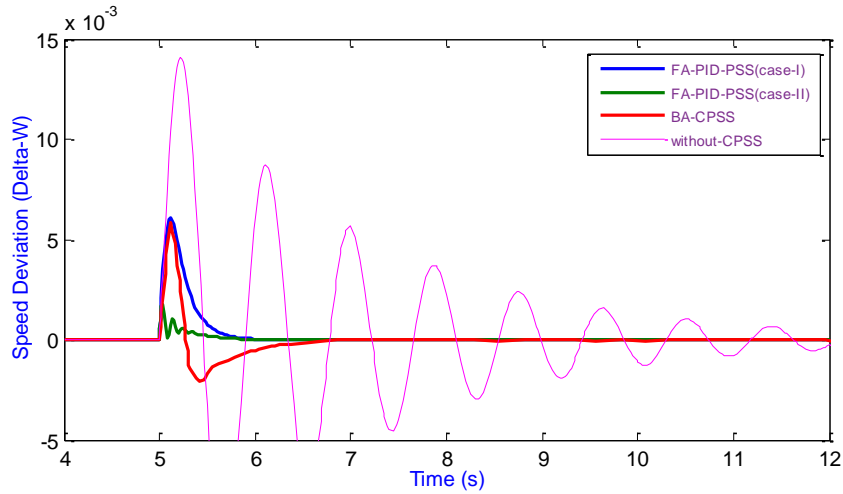


Figure 12. Speed response of without PSS, FA-PID-PSSs (case-I, II) and BA-CPSS based SMIB power system for Condition -3.

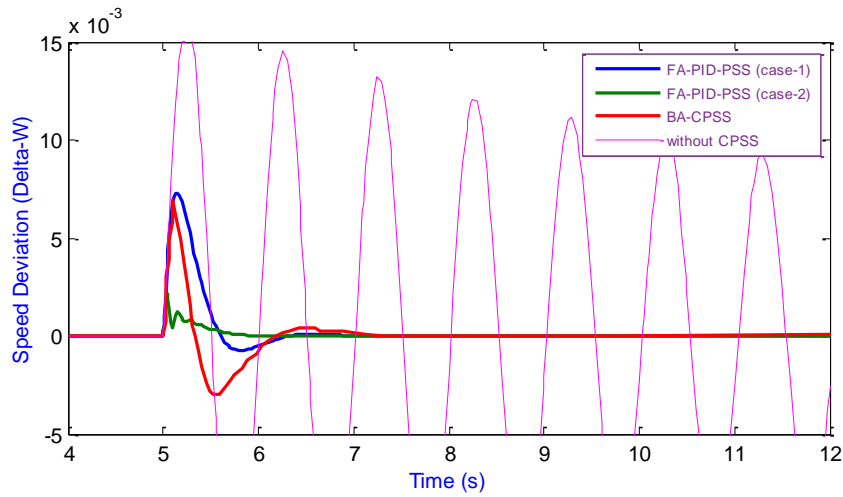


Figure 13. Speed response of without PSS, FA-PID-PSSs (case-I, II) and BA-CPSS based SMIB power system for Condition -4.

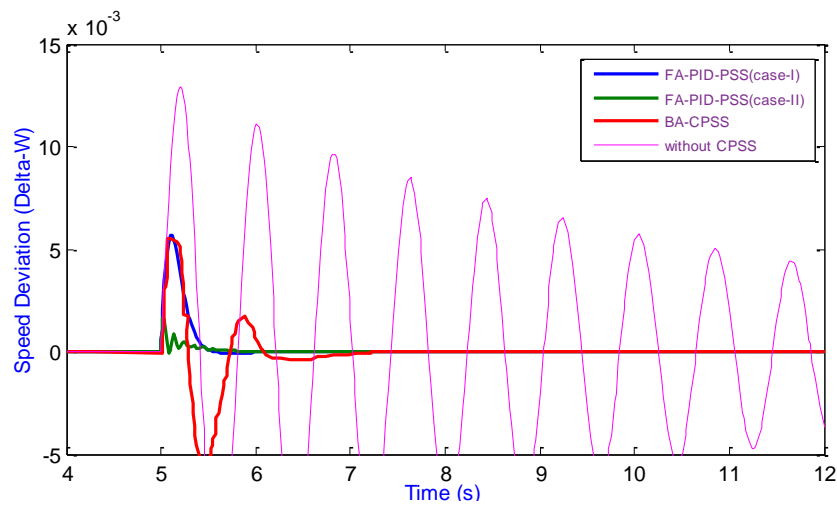


Figure 14. Speed response of without PSS, FA-PID-PSSs (case-I, II) and BA-CPSS based SMIB power system for Condition -5.

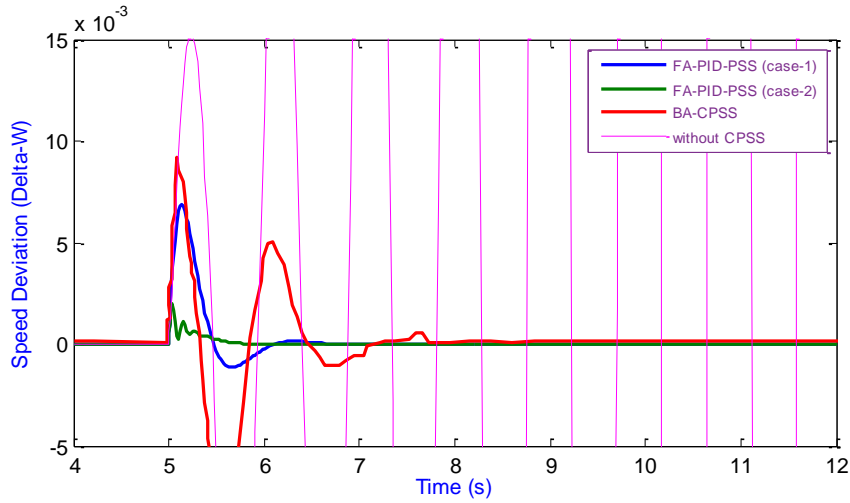


Figure 15. Speed response of without PSS, FA-PID-PSSs (case-I, II) and BA-CPSS based SMIB power system for Condition -6.

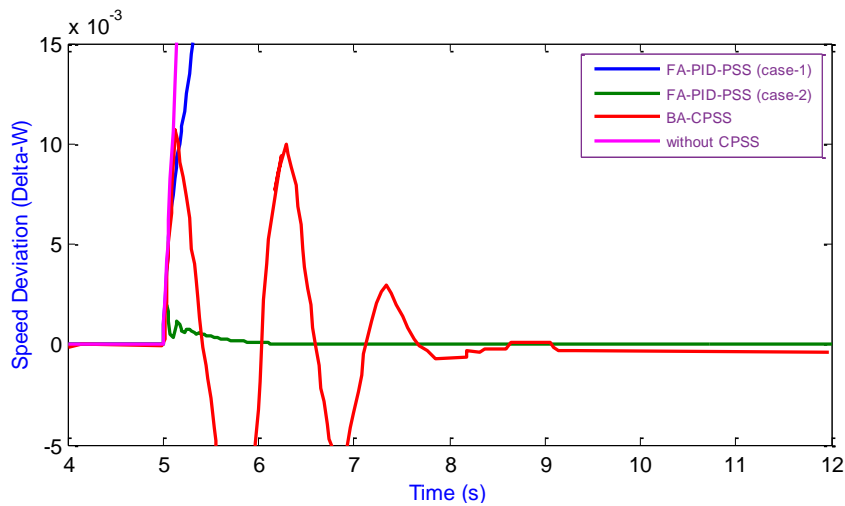


Figure 16. Speed response of without PSS, FA-PID-PSSs (case-I, II) and BA-CPSS based SMIB power system for Condition -7.

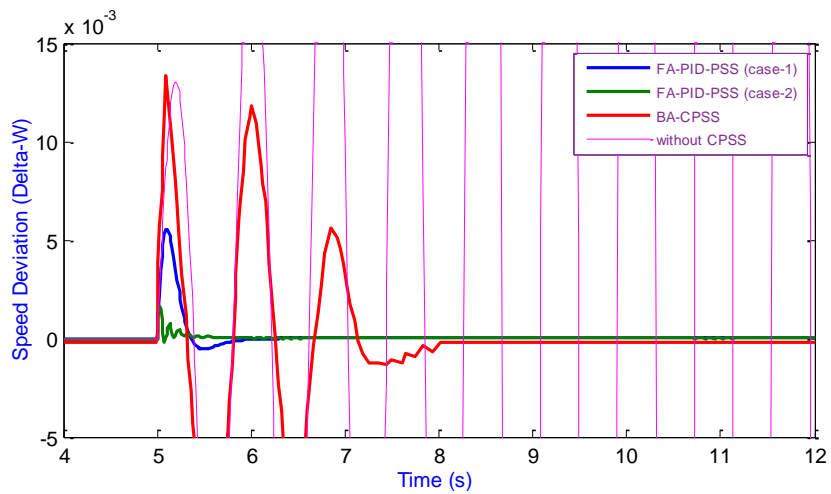


Figure 17. Speed response of without PSS, FA-PID-PSSs (case-I, II) and BA-CPSS based SMIB power system for Condition -8.

#### 4.5. Speed Response Analysis

The speed response of the SMIB power system for eight selected operating conditions are specified by simulation and also the comparison among the test systems are performed.

1. The test system without PSS.
2. The test system is equipped with BA-CPSS as in [9].
3. The test system is equipped with Firefly algorithm tuned PID- PSS (FA-PID-PSS) in cases-I and II.

The comparison result of speed response of the selected operating conditions 1–8 for all four forms are traced in Figures 10–17. According to the graphic results, the BA-CPSS based SMIB system has the ability to stabilize the speed response for all sample operating conditions, but with higher overshoots and long settling times as compared to FA-PID-PSS (case-I and II). Only for operating condition-7 the FA-PID-PSS of case-I isn't able to stabilize the speed response. The settling time and overshoot obtain for four states of each operating condition are enlisted in Table 6. Since, the oscillations of the system with FA-PID-PSS (case-II) are damped out much faster for all sample operating conditions as compared with BA-CPSS and FA-PID-PSS (case-I) based power system and also, FA-PID-PSS (case-II) is caused to reduces the overshoot of the speed deviation curve better than the others; indicates the best performance and superiority of FA-PID-PSS (case-II). Besides of it, according to eigenvalue analysis seven operating conditions with BA-CPSS and the same seven operating conditions with FA-PID-PSS (case-I) are unstable while all are stable with FA-PID-PSS (case-II).

**Table 6.** Settling time and overshoot for speed response with FA-PID-PSSs (case I,II) and BA-CPSS [9].

Power system Model	FA-PID-PSS (case-II)		FA-PID-PSS (case-I)		BA-CPSS		NO-PSS	
	settling time duration (s)	overshoot	settling time duration (s)	overshoot	settling time duration (s)	overshoot	settling time duration (s)	overshoot
Condition-1	1.06	0.002013	1.06	0.006957	2.72	0.004355	10.0	0.01592
Condition-2	1.10	0.002382	2.39	0.008515	2.39	0.004150	>12	0.01788
Condition-3	0.95	0.001722	0.95	0.006046	2.28	0.005828	>12	0.01397
Condition-4	1.00	0.002123	1.35	0.007306	2.30	0.006939	Oscillatory	increasing
Condition-5	1.14	0.001638	1.14	0.005671	2.42	0.005487	Oscillatory	increasing
Condition-6	0.94	0.001994	1.60	0.009859	2.46	0.00934	Oscillatory	increasing
Condition-7	0.94	1.30	unstable	unstable	4.02	0.01069	unstable	unstable
Condition-8	0.90	0.001629	1.25	0.005570	3.31	0.01335	Oscillatory	increasing

#### 5. CONCLUSION

In this study, the Firefly based PID-PSS is presented for the power system stability improvement. For two bounds PID parameters optimization is accomplished by using firefly algorithm by objective function based on eigenvalues. 133 different operating conditions have been taken to analyze the eigenvalues for the robust tuning of PSS. For eight sample operating conditions (1 to 8) the rotor speed responses have been analyzed. The speed responses of the rotors for the SMIB system without power system stabilizer, with BA-CPSS, with the FA-PID-PSS (case-I) and with the FA-PID-PSS (case-II) are compared for different operational conditions of power system models. According to the eigenvalue analysis and time response parameters like settling time and overshoot results, it is found that BA-CPSS and FA-PID-PSS (case-I) have the ability to stabilize the system for some operating conditions and aren't able to reduce the settling time duration and overshoot size; but the response with FA-PID-PSS (case-II) can stabilize the system and can improve settling time and overshoot for all operating conditions. Use of FA-PID-PSS (case-II) guarantees the small signal stability of SMIB system because all eigenvalues of electromechanical modes (for 133 operating conditions) are shifted to left hand side of the s-plane D-shape sector while seven unstable operating conditions with BA-CPSS and FA-PID-PSS (case-I) based power system have been proved.

## Appendix A

### A.1. Data for SMIB power system

$$x_d = 1.97 \text{ pu}, X_q = 1.9 \text{ pu}, X'_d = 0.30 \text{ pu}, T'_{d0} = 6.84 \text{ s}, K_A = 100, T_A = 0.02 \text{ s}, E_{fd}^{\min} = -5 \text{ pu}, E_{fd}^{\max} = 5 \text{ pu}, \omega_0 = 2\pi \times 50 \frac{\text{rad}}{\text{sec}}.$$

## Acknowledgment

I. Eke is supported by The Scientific and Technical Research Council of Turkey (TUBITAK) Turkey, through the postdoctoral research program 2219, under application number 1059B191300593. And Scientific Research Projects Coordination Unit (BAP - project number 2012/112 ) of Kirikkale University (TUBITAK).

## CONFLICTS OF INTEREST

No conflict of interest was declared by the authors.

## REFERENCES

- [1] Kamari, N. A., Musirin, I., Othman, M. M. and Hamid, Z. A., "PSS-LL Based Power System Stability Enhancement Using IPSO Approach", IEEE 7th International Power engineering and Optimization conference (PEOCO2013), Page(s): 658 – 663, (2013)
- [2] Shubhanga, Dr. K. N., Yadi Anantholla, Mr. "Manual for A Multi-machine Small-signal Stability Program", Version-1, India.
- [3] Hingorani, N.G and Gyugyi, L., "Understanding FACTS", IEEE press, NewYork, Page(s): (425–429), (2000).
- [4] Abdul Jaleel, J., Thanvy, N., "A Comparative Study between PLPD,PID and Lead-Lag controllers for Power System Stabilizer" 2013 International Conference on Circuits, Power and Computing Technologies [ICCPCT-2013], India, (2013).
- [5] Demello, FP., Concordia, C. "Concepts of synchronous machine stability as affected by excitation control". IEEE Trans Power Apparatus System; PAS-88: 316–29, (1969).
- [6] Sebaa, K., Boudour, M., "Optimal locations and tuning of robust power system stabilizer using genetic algorithms". Electr Power Syst Res;79: 406–16, (2009).
- [7] Peng, Z., Malik, OP., "Design of an adaptive PSS based on recurrent adaptive control theory". IEEE Trans Energy Convers, 24:884–92, (2009).
- [8] Ramakrishna, G., Malik, OP., "Adaptive PSS using a simple on-line identifier and linear pole-shift controller". Electrical Power Syst Res; 80:406–16.[http:// dx.doi.org/10.1016/j.epr.2009.10.004](http://dx.doi.org/10.1016/j.epr.2009.10.004), (2010).
- [9] Sambariya, D.K., Prasad, R., "Robust tuning of power system stabilizer for small signal stability enhancement using metaheuristic bat algorithm" Electrical Power and Energy Systems, 61: 229–238, (2014).



- [10] EKE,I., TAPLAMACIOĞLU, M. C. ve KOCA ARSLAN, I., “Power System Stabilizer Design for Rotor angle stability”, *International Journal of Engineering Research and Development*, Vol.3, No.2, June (2011).
- [11] Al-Duwaish, H.N., Al-Hamouz, Z.M., “A neural network based adaptive sliding mode controller: application to a power syst stabilizer”. *Energy Convers Manage*; 52:1533-8, (2011).
- [12] Soliman, M., Elshafei A.L., Bendary, F., Mansour, W. LMI., “Static output-feedback design of fuzzy Sower System Stabilizers”. *Expert System Appl*; 36:6817–25, (2009).
- [13] Mukherjee, V., Ghoshal, SP., “Intelligent particle swarm optimized fuzzy PID controller for AVR system”, *Electrical Power System Res*; 77: 1689–98, (2007).
- [14] Bhati, PS., Gupta, R., “Robust fuzzy logic power system stabilizer based on evolution and learning”. *Int J Electrical Power Energy System*; 53: 357–66, (2013).
- [15] Saoudi, K, Harmas, MN., “Enhanced design of an indirect adaptive fuzzy sliding mode power system stabilizer for multi-machine power systems”. *Int. J. Electrical Power Energy System*; 54: 425–31, (2014).
- [16] Ghasemi, A., Shayeghi, H., Alkhatib, H., “Robust design of multi-machine power system stabilizers using fuzzy gravitational search algorithm”. *Int J. Electrical Power Energy System*; 51: 190–200, (2013).
- [17] Ramirez, JM., Correa, RE., Hernández, DC., “A strategy to simultaneously tune power system stabilizers”. *Int J. Electrical Power Energy System*; 43: 818–29, (2012).
- [18] Nechadi, E., Harmas, MN., Hamzaoui, A., Essounbouli, N., “A new robust adaptive fuzzy sliding mode power system stabilizer”. *Int J Electr Power Energy Sys*; 42: 1-7, (2012).
- [19] Chaturvedi, DK., Malik, OP., “Neurofuzzy power system stabilizer”. *IEEE Trans Energy Convers*;23: 887–94, (2008).
- [20] Awadallah, MA., Soliman, HM., “A neuro-fuzzy adaptive power system stabilizer using genetic algorithms”. *Electr Power Compon Syst*; 37: 158–73, (2009).
- [21] Radaideh, SM., Nejdawi, IM., Mushtaha, MH., “Design of power system stabilizers using two level fuzzy and adaptive neuro-fuzzy inference systems”. *Int J Electr Power Energy System*; 35: 47–56, (2012).
- [22] Chaib, L., Choucha, A. Arif, S., “Optimal design and tuning of novel fractional order PID power system stabilizer using a new metaheuristic Bat algorithm”. *Ain Shams Engineering Journal* 8: 113–125, (2017).
- [23] Soliman, M., Elshafei, A.L., Bendarya. F., Mansour, W., “Robust decentralized PID-based power system stabilizer design using an ILMI approach”. *Electr Power Syst Res*; 80: 1488–97, (2010).
- [24] Soliman, M., “Parameterization of robust three-term power system stabilizers”. *Electr Power Syst Res*; 117: 172–84, (2014).
- [25] Yanwei, C., Hui, Y., Huidang, Z., “PID controller parameters tuning in servo system based on chaotic particle swarm optimization”. In: *IT in Medicine & Education. ITIME '09. IEEE International Symposium on*, vol. 1, Page: 276–280, (2009).

- [26] Abdul-Ghaffar, H., Ebrahim, EA., Azzam, M., “Design of PID controller for power system stabilization using hybrid particle swarm-bacteria foraging optimization”. WSEAS Trans Power Syst; 8: 12–23, (2013).
- [27] Duman, S., Ozturk, A., “Robust design of PID controller for power system stabilization by using real coded genetic algorithm”. Int Rev Electr Eng, vol. 5, N. 5, page: 2159–70, (2010).
- [28] Gandhi, P.R., Joshi, S.K., “GA and ANFIS based Power System Stabilizer” Power and Energy Society General Meeting (PES); Page(s): (1 – 5), (2013).
- [29] Curtis, J., “Process control instrumentation technology”, Fourth Edition, PHI, (1998).
- [30] Akkawi, A.R., Ali, M.H., Lamont, L.A., El Chaar, L., “Comparative Study between Various Controllers for Power System Stabilizer using Particle Swarm Optimization”, Electric Power and Energy Conversion Systems (EPECS), 2011 2nd Int. Conference; Page(s): (1 – 5), (2011).
- [31] Khodabakhshian, A., Hemmati, R., “Multi-machine power system stabilizer design by using cultural algorithms”. Int J Electrical Power Energy System; 44: 571–80, (2013).
- [32] Yang, X. S., “Nature-Inspired Metaheuristic Algorithms”, Luniver Press, UK, (2008).
- [33] Agarwal, S., Singh, A.P., Anand, N., “Evaluation Performance Study of Firefly Algorithm, Particle Swarm Optimization and Artificial Bee colony algorithm for Non-Linear mathematical Optimization functions”, Computing, Communications and Networking Technologies (ICCCNT), 2013 4th Int. Conference, Page(s): (1–8), (2013) .
- [34] Yang, X. S., “Firefly algorithms for multimodal optimization”, Proc. 5th Symposium on Stochastic Algorithms, foundations and Applications, (Eds. O. Watanabe and T. Zeugmann), Lecture Notes in Computer Science, 5792: 169-178, (2009).
- [35] Yang, X. S., “Engineering Optimisation: An Introduction with Metaheuristic Applications”, John Wiley and Sons, USA, (2010).
- [36] Kundur, P., Power system stability and control. 12<sup>th</sup> reprint. New Delhi, India, Tata McGraw-Hill Education Pvt. Ltd., (2011).